Motility of Single One-Headed Kinesin Molecules Along Microtubules

Yuichi Inoue,* Atsuko Hikikoshi Iwane,† Takayuki Miyai,† Etsuko Muto,‡ and Toshio Yanagida*†
*Single Molecule Processes Project, ICORP, and ‡Form and Function Group, PRESTO, JST, Osaka 562-0035, and †Department of Physiology and Biosignaling, Graduate School of Medicine, Osaka University, Osaka 565-0871, Japan

ABSTRACT The motility of single one-headed kinesin molecules (K351 and K340), which were truncated fragments of *Drosophila* two-headed kinesin, has been tested using total internal reflection fluorescence microscopy. One-headed kinesin fragments moved continuously along the microtubules. The maximum distance traveled until the fragments dissociated from the microtubules for both K351 and K340 was ~600 nm. This value is considerably larger than the space resolution of the measurement system (SD ≈ 30 nm). Although the movements of the fragments fluctuated in forward and backward directions, statistical analysis showed that the average movements for both K340 and K351 were toward the plus end of the microtubules, i.e., forward direction. When BDTC (a 1.3-S subunit of *Propionibacterium shermanii* transcarboxylase, which binds weakly to a microtubule), was fused to the tail (C-terminus) of K351, its movement was enhanced, smooth, and unidirectional, similar to that of the two-headed kinesin fragment, K411. However, the travel distance and velocity of K351BDTC molecules were ~3-fold smaller than that of K411. These observations suggest that a single kinesin head has basal motility, but coordination between the two heads is necessary for stabilizing the basal motility for the normal level of kinesin processivity.

INTRODUCTION

Conventional kinesin is a heterodimer consisting of two light chains and two heavy chains that converts the chemical energy derived from ATP hydrolysis into mechanical work as vesicle transport and membrane motility (Bloom and Endow, 1995). Recent x-ray crystallography has revealed the atomic structure of the kinesin catalytic domain, i.e., the N-terminal domain consisting of ~330 amino acids, including the ATP- and microtubule-binding sites (Kull et al., 1996; Sack et al., 1997). Mutant analysis has demonstrated that the ~15-amino-acid sequence following the catalytic domain, called the neck linker, determines the directionality of the kinesin movement (Endow and Waligora, 1997; Henningsen and Schliwa, 1997; Case et al., 1997).

A property of conventional kinesin is that individual molecules can processively move along microtubules over long distances up to several microns without dissociating. Processive movement of single two-headed kinesin molecules was directly observed in in vitro motility assays (Howard et al., 1989; Block et al., 1990; Vale et al., 1996). The processivity for two-headed kinesin was also supported by the kinetics of microtubule-activated kinesin ATPase, showing that two-headed kinesin hydrolyzes ~100 ATP molecules per encounter with the microtubules (Hackney, 1995).

The processive motility of kinesin has been explained by a hand-over-hand model, in which one head remains bound to the microtubule while the other detaches and moves forward (Cross, 1995). This model has been supported by several recent studies. Biochemical assays showed the alternating head catalysis in which two heads of kinesin hydrolyze ATP in a cooperative manner (Hackney, 1994). Structural studies have demonstrated conformational changes in the neck linker that may lead the partner head in the forward direction to the plus end of the microtubule (Rice et al., 1999). It has been reported that single one-headed kinesin molecules cannot processively move along a microtubule, although multiple one-headed kinesin molecules can drive microtubules (Berliner et al., 1995; Vale et al., 1996; Hancock and Howard, 1998), suggesting that the two-headed structure is essential for kinesin processive motility.

Some recent observations, however, do not necessarily support the hand-over-hand model. The atomic structure of dimeric kinesin with bound ADP shows that the two heads cannot simultaneously bind to the respective binding sites on a microtubule unless the dimer is highly strained (Kozielski et al., 1997). A single KIF1A molecule, which is a monomeric member of the kinesin-related proteins, can move continuously along microtubules (Okada and Hirokawa, 1999). Furthermore, biochemical studies show that truncated one-headed kinesin hydrolyzes 3–28 ATP molecules per encounter with microtubules (Jiang et al., 1997; Okada et al., 1999), indicating biochemical processivity of one-headed kinesin.

In our previous study, we tested the motility of one-headed kinesin using laser-trapping nanometry and showed that a small number of one-headed kinesin molecules, pos-

Received for publication 20 April 2001 and in final form 18 July 2001.

Y. Inoue's present address: Department of Biological Sciences, Graduate School of Science, University of Tokyo, Hongo, Tokyo 113-0033, Japan.

E. Muto's present address: Developmental Brain Science Group, RIKEN Brain Science Institute (BSI), 2–1 Hirosawa, Wako, Saitama 351-0198, Japan.

Address reprint requests to Dr. Toshio Yanagida, Osaka University, Graduate School of Medicine, Department of Physiology and Biosignaling, Osaka 565-0871, Japan. Tel.: 81-6-6879-3621; Fax: 81-6-6879-3628; E-mail: yanagida@phys1.med.osaka-u.ac.jp.

0006-3495/01/11/2838/13 $2.00

sibly one, attached to a bead could processively move along a microtubule (Inoue et al., 1997). However, it was difficult to demonstrate that the number of molecules attached to a bead was indeed one. Recently, we have developed a new assay system in which the movement of single fluorescently labeled kinesin along a microtubule can be directly observed using total internal reflection fluorescence microscopy (Vale et al., 1996; Miyamoto et al., 2000). In this study, we have measured the movement of single fluorescently labeled one-headed kinesin, which was a truncated fragment of *Drosophila* two-headed kinesin, along microtubules using total internal reflection fluorescence microscopy coupled with computer-based image analysis. Single one-headed kinesin fragments traveled continuously for several hundred nanometers along a microtubule in both forward and backward directions. Statistical analysis showed that the movement of a one-headed fragment was biased to the forward direction. Fusion of the tail of one-headed kinesin with BDTC, which binds weakly to a microtubule, enhanced the movement, making it more similar to the processive movement observed with two-headed kinesin. These observations suggest that a single kinesin head has basal motility and the second head may act as a stabilizer for ensuring processive movement.

MATERIALS AND METHODS

Chemicals and other materials

Malachite Green and casein were obtained from Nakarai Tesque (Kyoto, Japan) and PEM, PIPES, EDTA, and EGTA were obtained from Dojindo Laboratories (Kumamoto, Japan). Cy3 and Cy5 were obtained from Amersham Pharmacia Biotech UK (Poole, UK). Other chemicals were obtained from Sigma Chemical Co. (St. Louis, MO).

Protein expression and purification

K340, K351, and K411 were prepared as previously described (Inoue et al., 1997) and labeled with Cy3. The *Drosophila* kinesin fragments of the N-terminal 340, 351, and 411 amino acid sequences with a reactive cysteine residue, respectively, were expressed in *Escherichia coli*, JM109 as fusions with glutathione S-transferase (GST). They were then purified by a glutathione-agarose and the affinity for microtubules. GST was removed (>99%) by proteolysis with thrombin, and kinesin fragments were labeled with Cy3-maleimide at their C-terminus. Kinesin fragments fused with BDTC were also prepared for K351 and K411 and fluorescently labeled at the reactive cysteine residue between the kinesin sequence and BDTC (K351BDTC and K411BDTC). The amino acid sequence of K351BDTC is as follows: *MAEREIPAEDSIKVVCRFRPLNDSEEKAGSKFVVKFPNNVEENCISIAGKVYLFDKVFKPNASQEKVYNEAAKSIVTDVLAGYNGTIFAYGQTSSGKTHTMEGVIGDSVKQGIIPRIVNDIFNHIYAMEVNLEFHIKVSYYEIYMDKIRDLLDVSKVNLSVHEDKNRVPYVKGATERFVSSPEDVFEVIEEGKSNRHIAVTNMNEHSSRSHSVFLINVKQENLENQKKLSGKLYLVDLAGSEKVSKTGAEGTVLDEAKNINKSLSALGNVISALADGNKTHIPYRDSKLTRILQESLGGNARTTIVICCSPASFNESETKSTLDFGRRAKTVKNVVCVNEELTAEEWKRR*lgpggghrkCfkgtipfvdpgvthMKLKVTVNGTAYDVDVDVDKSHENPMGTILFGGGTGGAPAPAAGGAGAGKAGEGEIPAPLAGTVSKILVKEGDTVKAGQTVLVLEAMKMETEINAPTDGKVEKVLVKERDAVQGGQGLIKIGdleliegreasagiryryqisrefivtd.

The kinesin sequence in K351BDTC is shown in italics, and the linkers between the kinesin sequence, the reactive cysteine, and BDTC are shown in lowercase letters. A BDTC fragment with a cysteine residue was also expressed and prepared as described above. The BDTC fragment labeled with Cy3-maleimide was purified by gel filtration (NAP-5 Sephadex G-25 column, Pharmacia Biotech).

Fluorophore/peptide ratio

Concentrations of kinesin fragments were determined by Bradford and Lowry assay techniques using bovine serum albumin as the standard. The purity of kinesin fragments was estimated as >95% by Coomassie-stained SDS-polyacrylamide gel electrophoresis (SDS-PAGE) gels. The concentration of kinesin-bound Cy3 was determined by the absorbance at 550 nm and fluorescence of non-stained SDS-PAGE gels by FluorImager595 (Molecular Dynamics, Sunnyvale, CA). The Cy3/peptide ratio estimated from Cy3 and peptide concentrations for K340, K351, K351, K351BDTC, and K411BDTC was 0.7–1.2. For K411, a high Cy3/peptide ratio of >0.3 caused the inactivation of motility. Therefore, for the K411 fragment, a Cy3/peptide ratio between 0.2 and 0.3 was used.

Sucrose density gradient centrifugation

The oligomeric states of kinesin fragments in a solution containing 20 mM K-PIPES (pH 6.8), 10 mM K-acetate, 4 mM $MgSO_4$, 2 mM EGTA, and 0.2 mM EDTA were examined using 5–20% sucrose gradient centrifugation with standard proteins of bovine serum albumin, ovalbumin, and carbonic anhydrase. Peak fractions of the standards were determined by densitometry of Coomassie-stained SDS-PAGE gels and fitted with a single Gaussian curve. Sedimentation coefficients were determined from a linear regression of the fraction number versus the S value.

ATPase assays

The microtubule-activated ATPase of the kinesin fragments was measured at 25°C in a solution containing 20 mM K-PIPES, 10 mM K-acetate, 4 mM $MgSO_4$, 2 mM EGTA, 0.2 mM EDTA, 0.2 mg/ml casein, and 40 μM Taxol using a modified Malachite Green method (Iwatani et al., 1999).

Polarity-marked microtubules

Tubulin was purified from bovine brain and labeled with Cy5 as previously described (Higuchi et al., 1997). Polarity-marked microtubules were prepared by polymerizing dimly labeled tubulin molecules onto the end of brightly labeled microtubule seeds (Hyman et al., 1991). Because the plus ends of the microtubules grow faster than minus ends, the longer dimly labeled segment (10.4 $\pm$ 3.1 μm, mean $\pm$ SD, $n = 25$) could be distinguished as the plus end from the shorter dimly labeled segment (0.5 $\pm$ 0.4 μm, mean $\pm$ SD, $n = 25$) at the minus end. This polarity of the microtubules was reconfirmed by a microtubule gliding motility assay driven by two-headed kinesin molecules adsorbed on the glass surface. For the microtubules with a total length of >10 μm and having >3-fold disparity in the plus- and minus-end lengths (for dimly labeled segments), the probability that the shorter dimly labeled segment is in the leading direction of the movement was >99%.

Single-motor motility assays

Single-motor motility assays were performed according to the method of Vale and colleagues (Vale et al., 1996; Miyamoto et al., 2000) with some modifications. To increase the binding affinity of kinesin fragments to the microtubules, a solution of low ionic strength was used (20 mM K-PIPES,

10 mM K-acetate, 4 mM $MgSO_4$, 2 mM EGTA, 0.2 mM EDTA, and 40 μM Taxol). Cy5-labeled microtubules (20 μg/ml) were applied to a flow chamber (dimensions, 25 μm $\times$18 mm $\times$ 9 mm) and adsorbed onto a cleaned quartz slide. The glass surface was then coated with 5 mg/ml casein to avoid nonspecific binding of kinesin fragments. After unbound casein was washed out with the buffer solution, Cy5-microtubules were combined with kinesin fragments in the buffer solution containing 1 mM ATP, 0.5% mercaptoethanol, and an oxygen scavenger system (Harada et al., 1990) at 25°C. In these experiments, kinesin concentrations of 0.1–10 nM were chosen so that individual molecules could be observed on a microtubule without overlap. When we applied 2 nM, 6 nM, and 1 nM K411, K351, and K340, respectively, the binding rates of kinesin fragments were 3.8 $\pm$ 0.7, 2.9 $\pm$ 0.6, and 8.2 $\pm$ 0.7 events/min/μm of microtubule (mean $\pm$ SD, $n = 10$ microtubules), respectively. Nonspecific binding of kinesin fragments to the casein-coated glass surface occurred at a rate of <0.5 events/min/corresponding area in the absence of microtubules. The photobleaching rate of kinesin attached to the glass surface was 0.02–0.1/s (maximum rate, 0.10 $\pm$ 0.01/s), which was slower than the detachment rate of 0.43–1.1/s for kinesin fragments. The kinesin dissociation constant, k_{rel}, was corrected with the observed rate of disappearance, k_{obs}, and the rate of photobleaching, k_{dis}, described as $k_{obs} = k_{rel} + k_{dis}$ (Romberg et al., 1998).

Optics

An area ~50 $\times$ 80 μm^2 was illuminated by a green laser (532 nm, Crystalaser) using total internal reflection fluorescence microscopy (Funatsu et al., 1995). Fluorescence of Cy3 was filtered by the combination of high-pass (transmission wavelength > 560 nm; Asahi Spectra Co., Tokyo, Japan) and low-pass filters (transmission wavelength = 380–630 nm; Asahi Spectra Co.) and imaged by a GenIV image intensifier (VH4–1845, Videoscope) coupled with an silicon intensified target or charge coupled device camera (Hamamatsu Photonics, Shizuoka, Japan) at video rate. The location of Cy5-labeled microtubules was identified by removing the low-pass filter. After contrast enhancement by an Argus-20 image processor (Hamamatsu Photonics), the image was recorded using a digital video recorder DSR-20 (Sony, Tokyo, Japan) for later analysis.

Image analysis

Image analysis was performed on a Macintosh computer using the public-domain program NIHimage with a custom macro. Fluorescence intensities were obtained using a rolling eight-frame average, which reduced the fluctuations by summing the intensities from an 8 $\times$ 8 pixel window and subtracting the background intensity. The intensities were measured within 3 s of the onset of illumination, so that >86% of fluorophores were observed before photobleaching. Because photobleaching caused an approximately equal stepwise decrease in intensity up to four steps (Vale et al., 1996), the fluorescence intensities of one to four dye molecules were in the linear range of the camera.

The positions of the single kinesin fragments were measured from the centroids of the fluorescent spots. Standard deviations of the position of kinesin fragments rigidly attached to the glass surface were 25–35 nm. The disappearance of the fluorescent intensity over two frames was scored as the kinesin detaching from the microtubules. Mean velocities for the entire population were estimated from the pairwise distances in which the traces were shifted by 2 (66 ms) or 20 frames (660 ms). The distances between the original and shifted traces were calculated every 33 ms. Statistical analysis was performed using computer software, StatView (SAS Institute, Cary, NC).

Microtubule-affinity assay of Cy3-BDTC

Cy3-BDTC (10 μM; Cy3/peptide = 1.0) was mixed with 0–11 μM microtubules for 60 min at 25°C and then centrifuged. The binding of Cy3-BDTC to microtubules was measured by absorbance readings at 550 nm for both the supernatant and precipitate of the centrifugation. This binding was also shown by SDS-PAGE. The fluorescence in the SDS-PAGE gel was also imaged by FluorImager595 (Molecular Dynamics) before staining.

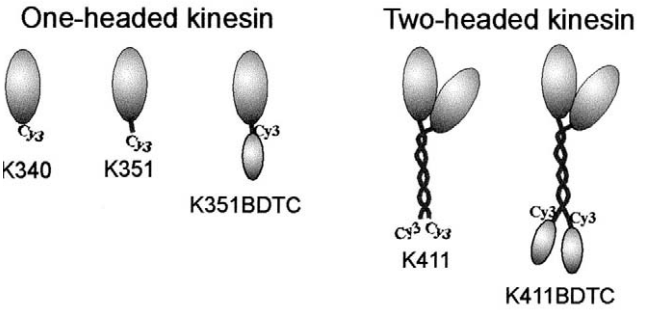

FIGURE 1 Illustrations of recombinant kinesin fragments. K340, K351, and K411 are *Drosophila* kinesin fragments having a reactive cysteine with the fluorescent dye, Cy3, attached. K351BDTC and K411BDTC are fragments fused with BDTC connected with the linker of a sequence of ~25 amino acids in which the reactive cysteine residue is fluorescently labeled with Cy3. Kinesin fragments are labeled with Cy3 in a molar ratio of 0.7–1.2, except for K411.

RESULTS

Oligomeric states in solution

Truncated kinesin fragments from *Drosophila* kinesin sequences were prepared as shown in Fig. 1. N-terminal fragments, K340, K351, and K411 were truncated at amino acid residues 340, 351, and 411, respectively, and attached to the C-terminus to which a reactive cysteine was fused (Inoue et al., 1997). To investigate the oligomeric state of kinesin fragments in solution, sucrose density gradient centrifugations were performed, using similar buffer conditions for single-motor motility assays (see Materials and Methods). Sedimentation coefficients of K340, K351, and K411 (Table 1) were consistent with previous reports (Correia et al., 1995; Jiang et al., 1997) in which K340 and K351 existed as monomers, whereas K411 formed a dimer. In the single-motor motility assay, the concentration of kinesin fragments, 0.1–10 nM, was more than 100-fold lower than that in the sucrose density gradient centrifugations. Therefore, during the motility assay it is unlikely that K340 and K351 formed dimers in solution.

Fusions of the proteins of K351 with BDTC (1.3-S subunit of *Propionibacterium shermanii* transcarboxylase) (Iwane et al., 1997) and K411 with BDTC were also prepared. The sedimentation coefficient for K351BDTC was significantly smaller than that of K411BDTC. Thus, K351BDTC and K411BDTC are thought to exist as monomers and dimers, respectively. The oligomeric states of kinesin fragments on the microtubules were also confirmed

TABLE 1 Biochemical and motile properties for the entire population of kinesin fragments

Fragment	Molecular mass (kDa)*	$S_{20,w}$ (S)†	Oligomeric state‡	V_{max} (/s)§	$K_{0.5(MT)}$ (μM)¶	Mean velocity (nm/s)‖	Duration of interaction (s)**	Mean travel distance (nm)††
K340	39	3.5	Monomer	73	0.017	31 ± 5 (902)	0.76 ± 0.09 (446)	32 ± 9 (505)
K351	39	3.5	Monomer	66	2.6	40 ± 3 (1260)	0.98 ± 0.07 (458)	38 ± 8 (525)
K351BDTC	57	4.3	Monomer	27	0.32	161 ± 2 (8222)	1.6 ± 0.2 (103)	362 ± 51 (103)
K411	46	4.6	Dimer	24	0.19	570 ± 7 (1841)	2.0 ± 0.3 (144)	1380 ± 120 (184)
K411BDTC	63	5.4	Dimer	30	0.19	526 ± 7 (1873)	1.8 ± 0.2 (188)	1310 ± 110 (225)

The values for V_{max} and $K_{0.5(MT)}$ were averaged from three to five different measurements. Mean velocities were estimated from the pairwise distances for 20 frames (660 ms), which were similar to those for 2 frames (data not shown).

*Molecular masses calculated from the amino acid sequence.

†Sedimentation coefficients averaged from two to four different experiments.

‡Oligomeric states determined both in solution and on the microtubules (see text).

§Maximum microtubule-stimulated ATPase rates.

¶Tubulin dimer concentrations giving half-maximal ATPase rates.

‖Mean ± SE; values in parentheses are the numbers of pairwise distances.

**Mean ± SE; values in parentheses are the numbers of molecules (see text and Fig. 4).

††Mean ± SE; values in parentheses are the numbers of molecules (see text and Fig. 6).

using total internal reflection fluorescence microscopy (see below).

Single-motor motility assays

The movements of fluorescently labeled kinesin fragments on polarity-marked microtubules were directly observed using total internal reflection fluorescence microscopy according to the method of Vale and colleagues (Vale et al., 1996; Miyamoto et al., 2000). Fig. 2 *a* shows the video images for two K340 fragments on the microtubule in the presence of ATP. Movement of the upper K340 fragment over a distance of 500 nm was clearly observed, whereas movement of the lower K340 was not detectable. Fig. 2, *b* and *c*, shows trajectories of the K340 fragments. In the absence of ATP (Fig. 2 *b*), K340 fragments remained securely attached in the same position before detaching from the microtubules. The standard deviation of the displacements determined by the image analysis was 33 nm. Because the fragments should bind rigidly to the microtubules in the absence of ATP, this standard deviation may represent the space resolution of the present system. In the presence of ATP (Fig. 2 *c*), a significant fraction of the K340 fragments moved along the microtubules. The movement, however, was not smooth but fluctuated between forward and backward directions. The other one-headed fragment, K351, showed similar behaviors to that of K340 (Fig. 2 *d*). However, when K351 was fused with BDTC, the movement of K351 was greatly enhanced (Fig. 2 *e*). The majority of the fraction of K351BDTC moved smoothly and processively in one direction.

Two-headed K411 fragments moved smoothly and processively along microtubules (Fig. 2 *f*) as previously reported (Vale et al., 1996; Miyamoto et al., 2000). However, we also noticed that ~10% of the population did not move for reasons unknown. When K411 was fused with BDTC (Fig. 2 *g*), the fragments also moved smoothly and processively, but the distribution of the velocity was broader than that of K411.

Oligomeric states on microtubules

The oligomeric states of kinesin fragments on microtubules were examined by measuring the fluorescence intensities. Although our sedimentation analysis showed that K340, K351, and K351BDTC were monomers in solution, they could form dimers on microtubules because the local concentration of fragments could be increased on the microtubules. Fig. 3 *a* shows the distribution of the fluorescence intensities of K351 sparsely adsorbed on a glass surface. The intensity distribution could be fitted to two Gaussian curves. Taking into consideration a labeling molar ratio (Cy3/peptide) of 0.9, fractions of K351 that were singly, doubly, or nonlabeled were calculated from the distribution to be 76%, 14%, and 10%, respectively. The fraction of singly labeled K351, however, could have been underestimated, because in some cases, two fragments may have been located in close proximity to each other and within the space resolution of the present system.

Fig. 3 *b* shows the intensity distribution of K351 on the microtubules in the presence of ATP. The main Gaussian curve of the distributions for the entire population (*gray bars*) coincided with that of K351 on a glass surface (Fig. 3 *a*), indicating that most of the K351 fragments did not dimerize even on the microtubules. Even when the measurement of fluorescence intensities was limited to only those fragments that actually moved on microtubules (Fig. 3 *b*, *white bars*), the resultant distribution was similar; i.e., the majority are monomers with a single label. Similar results were obtained for K340 (data not shown).

For K351BDTC, the distribution of fluorescence intensities for those fragments moving on the microtubules (Fig. 3 *c*, *white bars*) was very similar to that of K351 (Fig. 3 *b*),

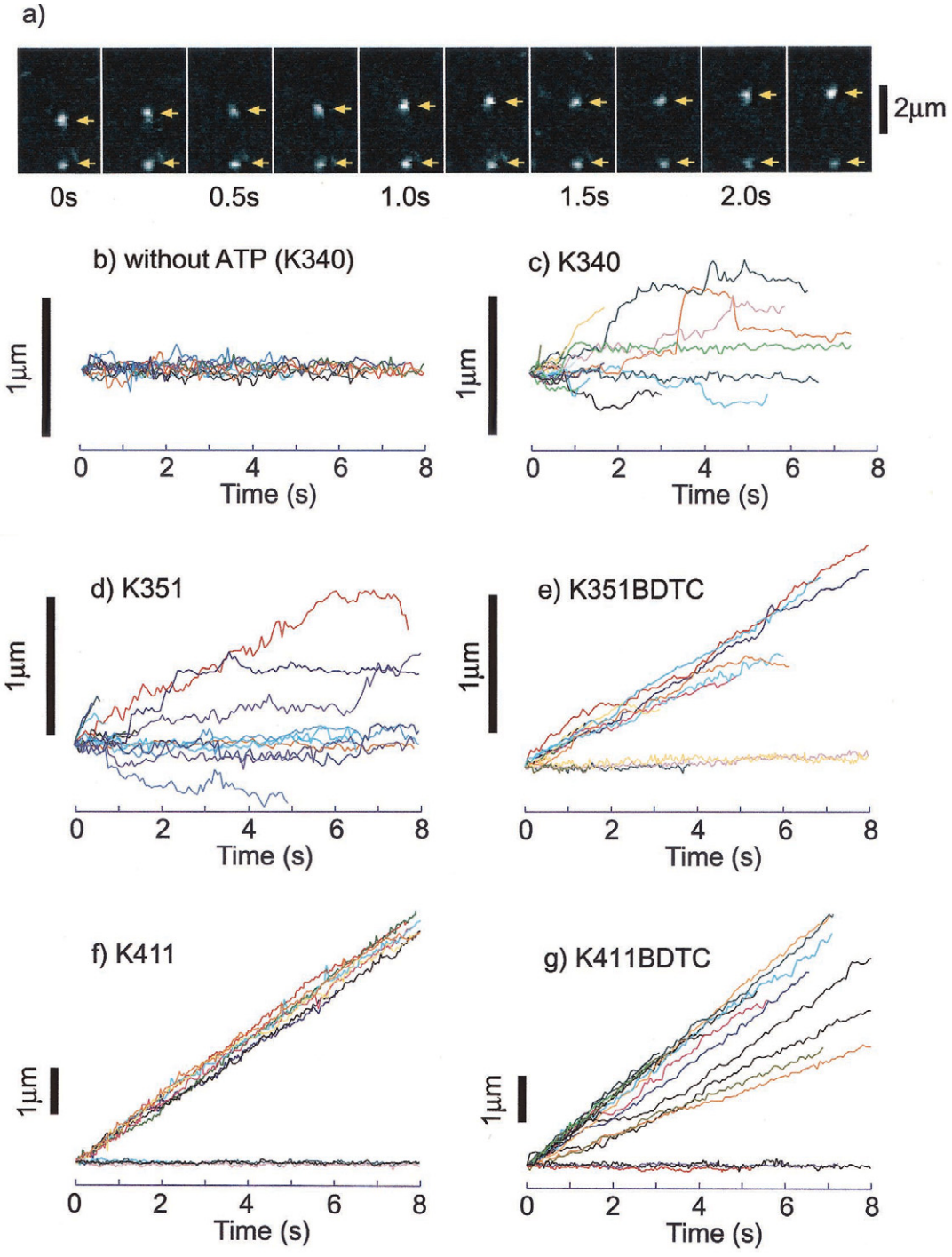

FIGURE 2 Movement of kinesin fragments along microtubules. (*a*) Sequential images of a single K340 molecule moving along a microtubule. Positions of the two K340 fragments are shown by arrows. The upper fragment moved, but the lower one remained at the same position (see text). [ATP] = 1 mM. (*b–g*) Time courses of the position of single kinesin fragments along microtubules. (*b*) Recordings made for K340 in the absence of ATP; (*c–g*) Recorded in the presence of 1mM ATP (*c*, K340; *d*, K351; *e*, K351BDTC; *f*, K411; *g*, K411BDTC). The position of kinesin fragments was determined by the centroids of the fluorescent spots (see Materials and Methods).

indicating that the majority of K351BDTC molecules were also monomers. In contrast, the distribution of fluorescence intensities for K411BDTC consisted of two major Gaussian curves, corresponding to a single and double fluorophore (Fig. 3 *d*). In addition, two minor Gaussian curves were detected, which most likely correspond to triple and quadruple fluorophores. Considering a labeling ratio of Cy3/peptide of 0.8, this distribution indicates that most of the

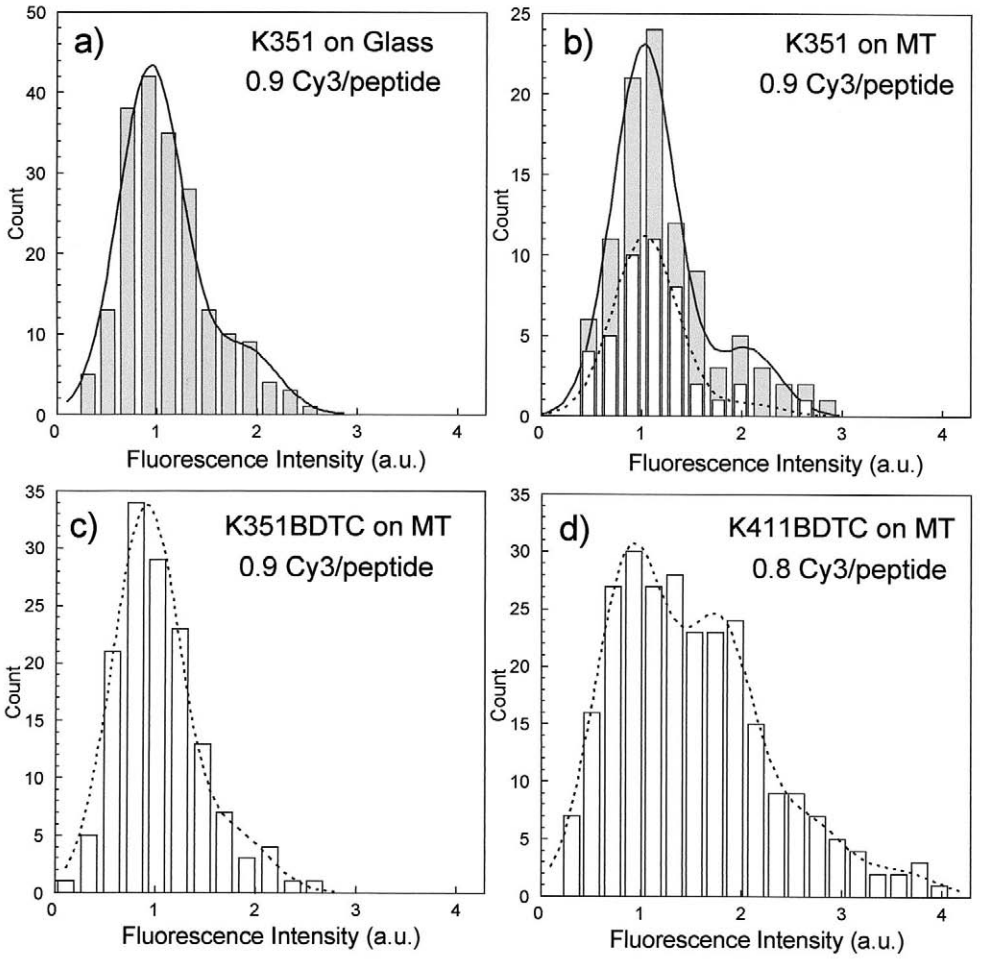

FIGURE 3 Histograms of the fluorescence intensities of kinesin fragments labeled with Cy3. Data have been fitted to Gaussian curves; $\Sigma C_i \times \exp[-(x - ix_1)^2/\sigma_1]$, where i (= 1, 2, 3, 4) is the number of Gaussian curves, Ci, x_1, and σ_1 are constants, and x is a variable. (*a*) Histogram of the fluorescence intensities of K351 sparsely adsorbed onto a glass surface. Data have been fitted by two Gaussian curves. Molar ratio of Cy3:K351 = 0.9:1. (*b*) Histograms of the fluorescence intensities of K351 interacting with microtubules in the presence of 1mM ATP. The distribution for the entire population of K351 fragments on the microtubules is shown by gray bars and has been fitted to two Gaussian curves (*solid line*). Distribution of the moving fraction of K351 fragments (see text) is shown by white bars and has been fitted to two Gaussian curves (*dotted line*). (*c*) Histogram of the fluorescence intensities of K351BDTC moving along microtubules. Data have been fitted to two Gaussian curves (*dotted line*). Molar ratio of Cy3:K351BDTC = 0.9:1. (*d*) Histogram of the fluorescence intensities of K411BDTC moving along microtubules. Data have been fitted to four Gaussian curves (*dotted line*). Molar ratio of Cy3:K411BDTC = 0.8:1.

K411BDTC fragments moving on the microtubules should be dimers (Vale et al., 1996). Therefore, we conclude that the oligomeric state of each kinesin fragments in the motility assay is same as that in the sedimentation analysis.

Analysis of the movement of the entire population of kinesin fragments

Some of the kinesin molecules, even the two-headed ones, did not move processively but remained attached to the microtubules (Fig. 2, *c–g*) with time courses similar to those obtained in the absence of ATP (Fig. 2 *b*). Because all fluorescent spots appearing in the fluorescent area of Cy5-MT were traced, these traces would also include molecules that had bound nonspecifically to the glass surface in close proximity to the microtubules. In some cases, however, it was very difficult to distinguish between the moving and nonmoving molecules, especially for K340 and K351, where the processivity was poor. Therefore, in the following analysis, we first focused on the motility of the entire population, which included the nonmoving molecules and the molecules bound nonspecifically to the glass.

Duration of interactions

Histograms for the durations of attachment of kinesin fragments to microtubules in the presence of ATP are shown in Fig. 4 (white bars). The mean durations have been estimated

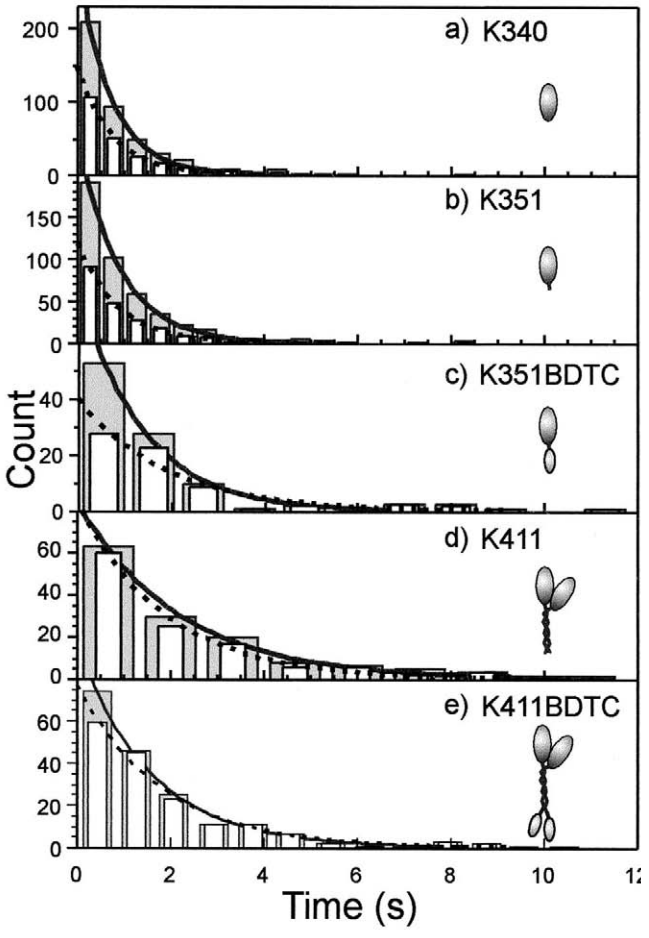

FIGURE 4 Duration of interaction with microtubules. Histograms show data for K340 (*a*), K351 (*b*), K351BDTC (*c*), K411 (*d*), and K411BDTC (*e*). The histograms for the entire population of kinesin fragments on the microtubules are shown by gray bars and have been fitted to single exponentials (*solid lines*). The distributions for the moving fractions (see text) are shown by white bars and have been fitted to the single exponentials (*dotted lines*). The time constants are shown in Tables 1 and 2 after correcting for photobleaching (see Materials and Methods).

from the best fit of single-exponential functions to the data after correcting for photobleaching (Romberg et al., 1998). The mean durations were 0.76 ± 0.09 s for K340 and 0.98 ± 0.07 s for K351, which were ~2-fold shorter than that of two-headed K411. The duration of K351 was increased by ~60% when fused with BDTC, whereas the duration of K411 was unaffected by the fusion of BDTC (Table 1).

Instantaneous and mean velocities

Distributions of the instantaneous velocities were obtained from the pairwise distances between 20 frames (Fig. 5, *gray bars*). In the absence of ATP (Fig. 5 *a*), where the kinesin fragments remained rigidly attached to microtubules, the distribution could be fitted to a single Gaussian curve with a peak of ~0 nm/s. In the presence of ATP, the distribution for two-headed K411 (Fig. 5 *e*, *gray bars*) was bimodal (Young et al., 1998) and could be well fitted to two Gaussian curves with peaks at ~0 nm/s and 672 nm/s. The major peak of the distributions for one-headed K340 and K351 (Fig. 5, *b–c*, *gray bars*) was observed at ~0 nm/s. However, a significant number of counts were observed in the velocity range of >200 nm/s, which were not observed in the absence of ATP. These distributions could also be fitted by two Gaussian curves with the second peak occurring at 33 and 58 nm/s for K340 and K351, respectively. For one-headed K351BDTC, the second peak at 261 nm/s was more clearly separated from the peak near 0 nm/s (Fig. 5 *d*, *gray bars*), indicating that the movement of K351 was accelerated by the fusion of BDTC. Interestingly, when BDTC was fused to two-headed K411, the distribution for K411BDTC showed a third peak at ~400 nm/s (Fig. 5 *f*, *gray bars*), which was not seen for K411. In contrast to the case of one-headed K351BDTC, it is possible that BDTC may cause friction during the movement of the two-headed fragment. The distribution for K411BDTC could be well fitted to three Gaussian curves with peaks at 0, 370, and 714 nm/s.

Mean velocities for the entire population are summarized in Table 1. In the presence of ATP, the mean velocities of K340 and K351 were 31 ± 5 and 40 ± 3 nm/s, respectively. These values were considerably higher than those obtained in the absence of ATP (2.4 ± 2.1 for K340, 0.3 ± 1.7 nm/s for K351). Student *t*-tests at the 99% significance level indicated that the probabilities for the hypotheses that the mean velocity = 0 were <0.001. Hence, one-headed kinesin fragments should have a bias, although small, to move toward the plus end of the microtubule. When K351 was fused with BDTC, the velocity of the one-headed fragment increased to 161 ± 2 nm/s (K351BDTC) but was still ~4 times smaller than the mean velocity of two-headed K411, 570 ± 7 nm/s. Unlike the case of one-headed kinesin, fusion of K411 with BDTC did not greatly change its mean velocity (526 ± 7 nm/s for K411BDTC).

In summary, all the species of kinesin fragments show a biased movement toward the plus end of the microtubule, and the general order of velocity was K411 ≥ K411BDTC > K351BDTC ≫ K351 ≥ K340.

Travel distance

Travel distances were directly measured for those fragments that associated with the microtubules (Fig. 6). In the presence of ATP, travel distances measured for K340 and K351 were distributed toward both the plus and minus ends of a microtubule (Fig. 6, *b* and *c*), and their distributions were broader than those in the absence of ATP (Fig. 6 *a*). Mean travel distances for K340 and K351 were 32 ± 9 nm and 38 ± 8 nm (mean ± SE, n = 505–525 molecules), respectively, which were both significantly larger than those in the

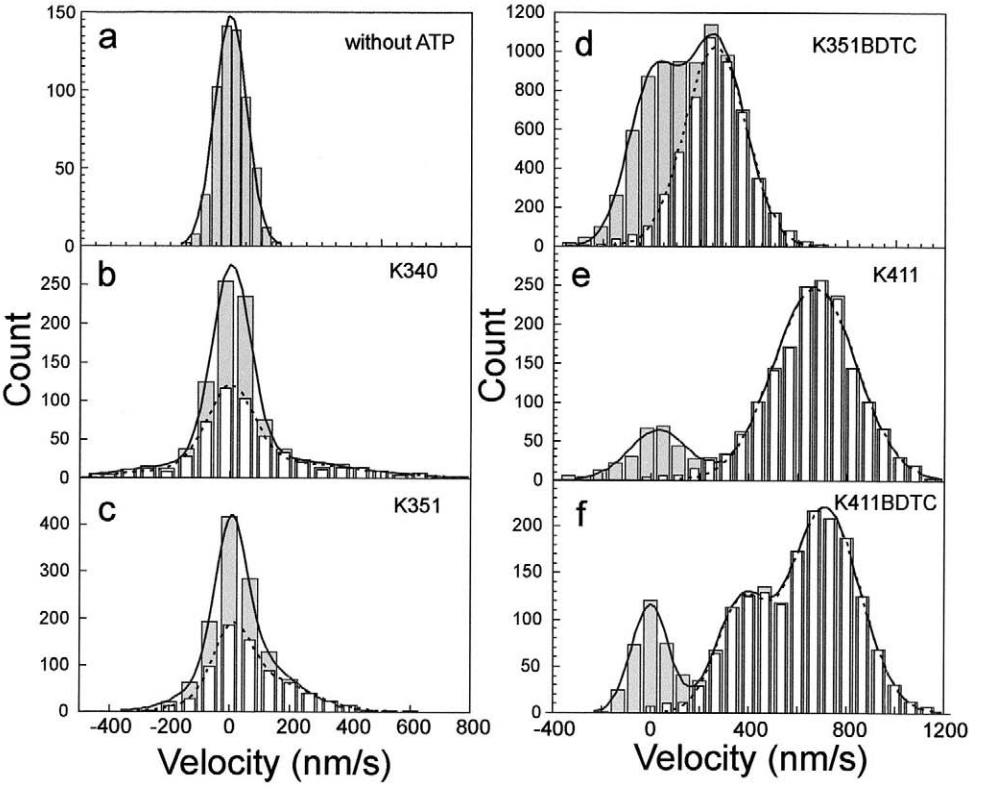

FIGURE 5 Distribution of the instantaneous velocity of kinesin fragments. Instantaneous velocities of kinesin fragments were calculated from the pairwise distances for 20 frames (see Materials and Methods). The histograms for the entire population of kinesin fragments on the microtubules are shown by *gray bars* and have been fitted to Gaussian curves (*solid lines*). The histograms for the moving fractions are shown by *white* bars and have been fitted to Gaussian curves (*dotted lines*). (*a*) K340 in the absence of ATP; solid line, single Gaussian curve. (*b–f*) In the presence of ATP. (*b*) K340; solid and dashed lines, double Gaussian curves. (*c*) K351; solid and dashed lines, double Gaussian curves. (*d*) K351BDTC; solid line, double Gaussian curves; dashed line, single Gaussian curve. (*e*) K411; solid line, double Gaussian curves; dashed line, single Gaussian curve. (*f*) K411BDTC; solid line, triple Gaussian curves; dashed line, double Gaussian curves.

absence of ATP (3.0 ± 3.1 nm). When K351 was fused with BDTC, travel distances were distributed predominantly toward the plus end of microtubules (Fig. 6 *d*) as observed for the two-headed fragments (Fig. 6, *e–f*), and they could be well fitted to a single-exponential function. The mean travel distance for K351BDTC (362 ± 51 nm) was increased ~10 times by the fusion of BDTC, although it is still fourfold smaller than that for two-headed K411 (1380 ± 120 nm) or K411BDTC (1310 ± 110 nm).

Analysis of the moving fraction of kinesin fragments

To further characterize the movement, we classified kinesin fragments into moving and nonmoving fractions as follows. Because the movement of one-headed K340 and K351 fluctuated in the forward and backward directions, we calculated the variance per duration of interaction (nm^2/s, VD) for each trace. In the absence of ATP, the VDs for K351 were less than 1500 nm^2/s. In the presence of ATP, however, the VDs for some fragments were more than 1500 nm^2/s. Thus, kinesin fragments whose VD was over 1500 nm^2/s have been classified as the moving fraction whereas those with a VD < 1500 nm^2/s were considered the nonmoving fraction. With this criterion, moving fractions for K340, K351, K351BDTC, K411, and K411BDTC were 49%, 56%, 66%, 87%, and 86%, respectively (Table 2).

Fig. 4 shows the histograms for the duration of interaction for the moving fraction (Fig. 4, *white bars*) and for the entire population (Fig. 4, *gray bars*). Mean values for the duration were determined from a single-exponential fit to the distributions after correcting for photobleaching (Romberg et al., 1998). The values for the duration of the moving fraction (shown in Table 2) were slightly larger than those for the entire population (shown in Table 1).

Fig. 5 shows the distribution of the instantaneous velocities for the moving fraction (Fig. 5, *b–f*, *white bars*) as well as for the entire population (Fig. 5, *b–f*, *gray bars*). For all kinesin constructs, the counts of the stationary kinesin fragments (with a velocity near 0 nm/s) were greatly reduced compared with the moving fraction, but the extent of reduction varied depending on the species of the kinesin constructs. For K351BDTC, K411, and K411BDTC, the peak at ~0 nm/s was greatly reduced and had almost disappeared (Figs. 5, *d–f*, *white bars*). However, for K340 and K351, the peak at ~0 nm/s, though significantly decreased, was still a major peak (Fig. 5, *b* and *c*, *white bars*). Because the movement of K340 and K351 was rather erratic, i.e., the molecules moved transiently and then stopped for short periods, the stationary phase contributed to the counts near 0 nm/s for the moving fraction of K340 and K351. The distributions of instantaneous velocities for K340 and K351 could be well fitted by two Gaussian curves, with peaks

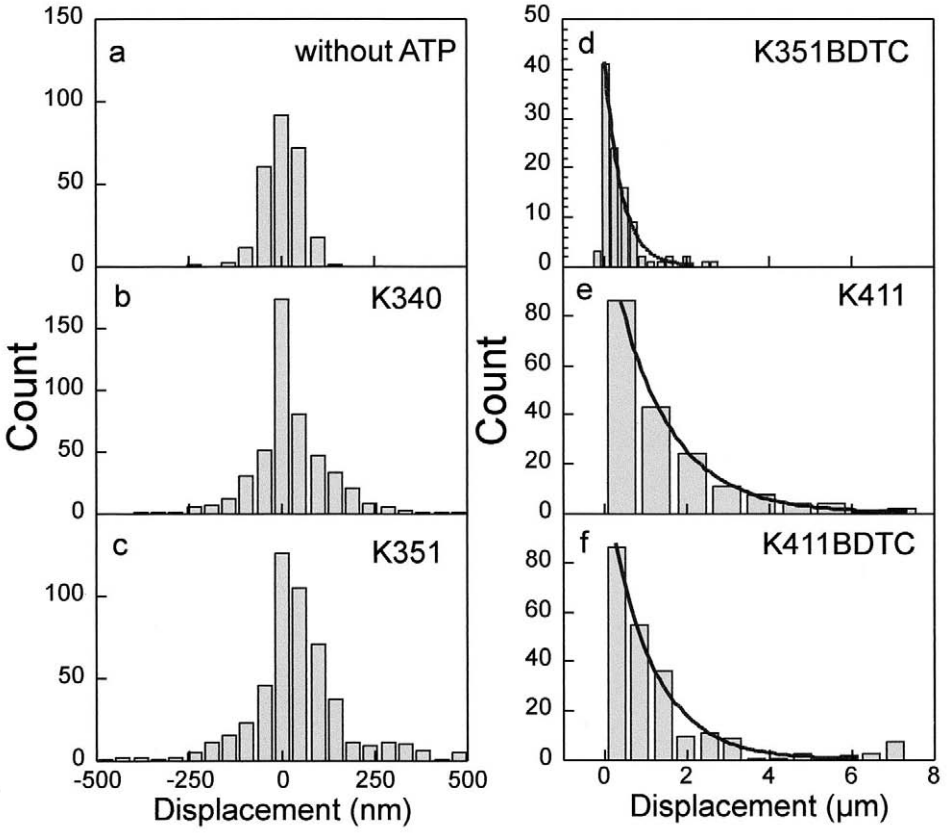

FIGURE 6 Histograms of the travel distances. The travel distances (distance between association and dissociation points) were directly measured for all fragments whose duration of interaction was >0.2s. The mean travel distances are summarized in Tables 1 and 2. (*a*) K340 in the absence of ATP; (*b* and *c*) Entire population of K340 and K351, respectively, in the presence of ATP; (*d–f*) Entire population of K351, K411, and K411BDTC, respectively, in the presence of ATP. Solid lines show a single-exponential fit to the data.

positioned at ~0 and 110 nm/s for K340, ~0 and 107 nm/s for K351. Mean velocities for the moving fraction of K340 and K351 were 51 and 67 nm/s, respectively, and were considerably slower than those of two-headed fragments (Table 2). However, it is important to note that one-headed K340 and K351, in the transient moving phase, moved at the same order of velocity for K351BDTC, K411, or K411BDTC.

Mean travel distance for the moving fraction was estimated from 70–335 fragments that moved over a distance of at least 60 nm toward the plus or minus end of the microtubule from the attached point (Table 2). Although this classification is not identical to that from the VD, the moving fractions were 42%, 64%, 68%, 88%, and 87% for K340, K351, K351BDTC, K411, and K411BDTC, respectively. These were similar to those obtained from the VD. Mean travel distances for K340 and K351 were 50–70% larger than those of the entire fraction. Because the classification of the moving fraction was independent of the moving direction, the results confirm that K340 and K351 have an average movement toward the plus end of the microtubules.

TABLE 2 Motile properties of the moving fraction of kinesin fragments

Fragment	Moving fraction*	Mean velocity (nm/s)†	Duration of interaction (s)‡	Mean travel distance (nm)§	Diffusion coefficient (mm^2/s)¶
K340	0.49	51 ± 8 (525)	0.81 ± 0.11 (238)	54 ± 10 (211)	9100
K351	0.56	67 ± 5 (710)	0.97 ± 0.12 (220)	58 ± 13 (335)	9600
K351BDTC	0.66	254 ± 2 (5017)	2.4 ± 0.3 (70)	531 ± 66 (70)	3000
K41	0.87	657 ± 5 (1579)	2.3 ± 0.2 (125)	1560 ± 130 (161)	6100
K411BDTC	0.86	625 ± 5 (1550)	2.2 ± 0.2 (167)	1490 ± 120 (196)	ND‖

Mean velocities were estimated from the pairwise distances for 20 frames (660 ms), which were similar to those for 2 frames (data not shown).
*Ratio of the number of moving fragments to that of all fragments associated with the microtubules (see text).
†Mean ± SE; values in parentheses are the numbers of pairwise distances.
‡Mean ± SE; values in parentheses are the numbers of molecules (see text and Fig. 4).
§Mean ± SE; values in parentheses are the numbers of molecules (see text).
¶Diffusion coefficients obtained from the linear fits to the variances in Fig. 7 *a*.
‖Not determined (see text).

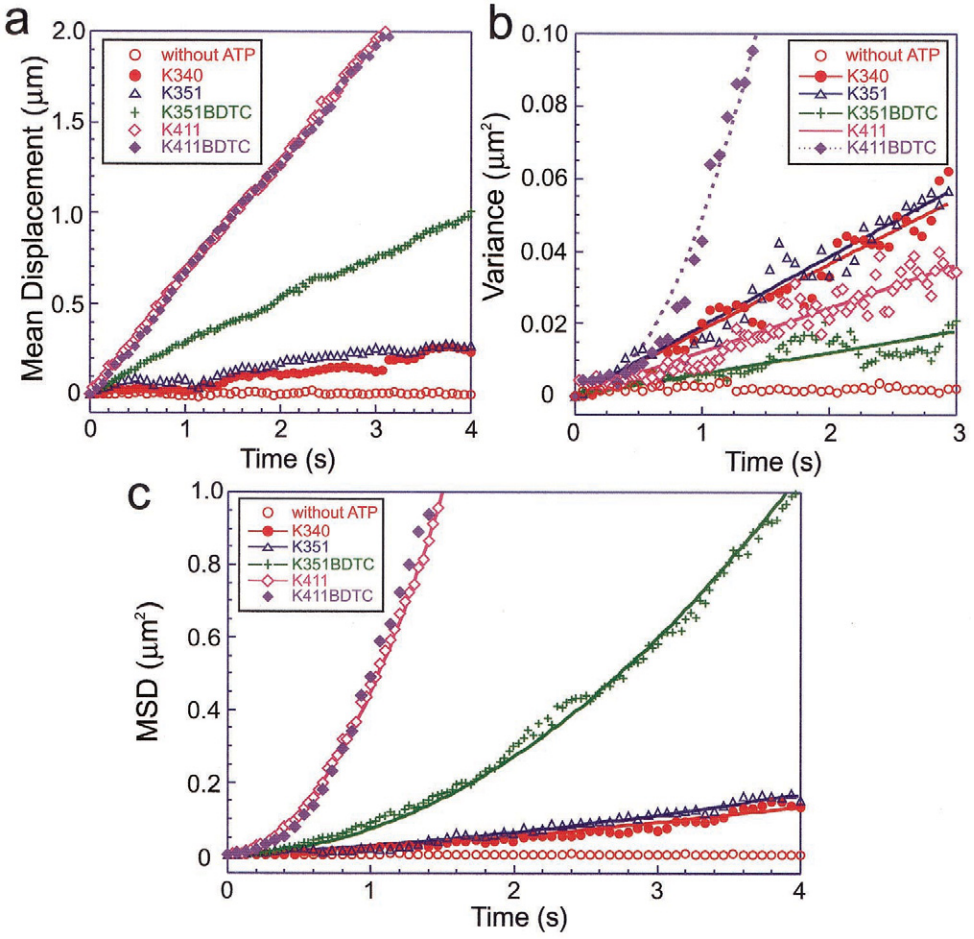

FIGURE 7 Analyses of the moving fractions of kinesin fragments. (*a*) Mean displacements. Time courses for the displacements of the moving fractions of K340 (●), K351 (△), K351BDTC (+), K411 (◇), and K411BDTC (◆), averaged for 30–40 fragments. For comparative purposes, the time courses of K340 in the absence of ATP (○) have also been averaged for 31 fragments. The mean velocities obtained from the linear fits to the mean displacements are 62, 76, 255, 651, and 638 nm/s for K340, K351, K351BDTC, K411, and K411BDTC, respectively. These values are consistent with those calculated from the pairwise distances (Table 2). (*b*) Mean variances. The time courses for the variances are calculated for 30–40 moving fragments and are shown as the same symbols in *a*. The variances of K340 in the absence of ATP are also shown for comparison (○). The variances for the moving K340, K351, K351BDTC, and K411 molecules increased with time in an approximately linear fashion. Diffusion coefficients (D) have been estimated from linear fits to the mean variances (*solid bars*; mean variance = $2Dt$) and summarized in Table 2. The diffusion coefficient of K411BDTC was not determined because the variance of K411BDTC increased with the square of the time (*dotted line*; mean variance = $0.049t^2$). (*c*) Mean square displacement (MSD). The time courses for the MSD have been calculated for 30–40 moving fragments and shown as the same symbols in *a*. The MSD of K340 in the absence of ATP is also shown. When the mean velocities (v) and the diffusion constants (D) estimated from *a* and *b*, respectively, are applied, the MSD plots for K340, K351, K351BDTC, and K411 could be well fitted with an equation for biased Brownian movement (*solid bars*; MSD (t) = $2Dt + v^2t^2$).

Analysis on the fluctuation of movement

Fig. 7 *a* shows the averaged time courses of displacements for the moving fractions. In the presence of ATP, the mean displacement for each species of fragment increased in a more or less linear fashion. In contrast, no change in the displacement was observed in the absence of ATP. The mean velocities obtained from the linear fits to the mean displacements (Fig. 7 *a*) were consistent with those calculated from the pairwise distances (*white bars* in Fig. 5, *b–f*, and Table 2).

The variances for K340, K351, K351BDTC, and K411 increased with time in an approximately linear fashion. Diffusion coefficients were obtained from the linear fit to the mean variance (Table 2). Diffusion coefficients for one-headed K340 and K351 were ~50% larger than that of two-headed K411. However, when fused with BDTC, the diffusion coefficient for K351BDTC was smaller than that of K411.

The variance of K411BDTC increased linearly with the square of time but not with time. This is consistent with the fact that the velocity of K411BDTC was widely spread and had an additional peak in the histogram showing the instantaneous velocities of the fragments (Fig. 5 *f*).

The stochastic nature of movement has been characterized by plotting mean square displacement (MSD) against

time (Okada and Hirokawa, 1999). The MSD plots of the moving fractions are shown in Fig. 7 *c*. The MSD plots for kinesin fragments could be well fitted with an equation for biased Brownian movement; MSD $(t) = 2Dt + v^2t^2$, where D is the diffusion coefficient estimated from Fig. 7 *b* and v is the mean velocity estimated from Fig. 7 *a*.

ATPase activity of kinesin fragments

Biochemical properties of kinesin fragments were examined by measuring microtubule (MT)-activated ATPase rates in the motility assay buffer (Table 1). All of the fragments had relatively high V_{max} values of 24–73/s, but one-headed K340 and K351 had higher values of 73 and 66/s, respectively. In contrast to the relatively similar V_{max} values, the microtubule concentration giving the half-maximum rate, $K_{0.5(MT)}$, differed dramatically over a 100-fold range. The $K_{0.5(MT)}$ value for one-headed K351 was ~14-fold higher than that for two-headed K411, whereas the $K_{0.5(MT)}$ for one-headed K340 was considerably lower. The pattern for the V_{max} and $K_{0.5(MT)}$ values was similar to those previously reported (Jiang et al., 1997; Huang and Hackney, 1994; Moyer et al., 1996; Ma and Taylor, 1997).

When BDTC was fused with K351, both V_{max} and $K_{0.5(MT)}$ values of K351BDTC approached those of two-headed K411. There was an eightfold decrease in the $K_{0.5(MT)}$ of K351 when BDTC was fused, indicating a significant increase in affinity. On the other hand, the kinetic properties of two-headed K411 were not significantly altered upon fusion with BDTC. These observations on the biochemical effects of BDTC were in parallel and consistent with the observations for motility.

The coupling between the ATP turnover and the 8-nm step of one-headed K340 and K351 differs from that of two-headed kinesin, which is tightly coupled in a one-to-one fashion (Schnitzer and Block, 1997; Hua et al., 1997). The ratio of V_{max} to the detachment rate from the microtubules observed in motility assays, 1.0–1.3/s, suggests that one-headed K340 and K351 fragments hydrolyze 56–66 ATP molecules before detaching from the microtubules. Because each such encounter yields on average (4–5) × 8 nm of progress, the coupling ratio of ATP turnover to an 8-nm step is ~10. This is probably because these fragments undergo forward and backward 8-nm steps frequently during movement or the coupling slips. When BDTC was fused to K351, the movement was smooth and the coupling was close to one to one.

DISCUSSION

Evidence for single one-headed molecules

It has been suggested that dimerization of *Drosophila* kinesin fragments occurs in the N-terminal fragments of more than 380 amino acid sequences (Huang et al., 1994; Correia., 1995). Oligomeric states of kinesin fragments were examined by sedimentation analysis as previously described (Inoue et al., 1997). Our results indicate that K340, K351, and K351BDTC exist as monomers, whereas K411 and K411BDTC form dimers. The design and oligomeric state examined here for K351BDTC and K411BDTC were similar to the previous report by Berliner and colleagues (Berliner et al., 1995; for monomer construct of 340BCCP and for dimer construct of 401BCCP). Furthermore, it has been suggested that K340, K351, and K351BDTC exist as monomers even on the microtubules under the conditions used for the single-motor motility assay, because the histograms of the fluorescence intensities on the microtubule were similar to those on the glass surface (Fig. 3).

In the single-motor motility assay, however, the possibility exists that the fragments, which have been photobleached or unlabeled, might dimerize with fluorescent fragments on the microtubules, and such dimers with only one fluorophore exhibit movement. This possibility was excluded for the following reasons.

First, because the detachment rate of K351 (1.0/s) was at least 10-fold faster than the photobleaching rate, the majority of K351 molecules that interacted with the microtubules should be observed before photobleaching occurred. If dimerization is essential for movement, then the moving fraction should be less than the unlabeled fraction (10% for K351 fragments). This is inconsistent with the results in this study where the moving fraction of K351 was 56%. Second, if fluorescently labeled K351 molecules form dimers with unlabeled molecules, then a significant number of fluorescently labeled K351 should also form dimers with labeled molecules. If this was the case, then the histogram of the fluorescence intensities for moving K351 should have a large peak corresponding to two dye molecules. However, the histogram for the moving fraction of K351 (white bars in Fig. 3 *b*) had a very small shoulder corresponding to the two dye molecules as observed for the entire population (gray bars in Fig. 3 *b*). Therefore, we conclude that moving fluorescent spots are indeed due to single one-headed molecules.

Single-headed processivity

Single-motor motility assays demonstrated that conventional one-headed kinesin, K340, and K351, having only one lysine residue at the K-loop site is much less processive than KIF1A and two-headed kinesin. Nevertheless, these molecules still exhibit small processive movements toward the plus end of the microtubule. These movements of one-headed fragments could be well fitted with the biased Brownian model proposed by Okada and Hirokawa (2000). The results indicate that the machinery essential for the processive movement is equipped in the minimal structure of K340, without any specific sequence such as a K-loop of KIF1A. The results from the raw traces (Fig. 2, *c* and *d*), as

well as in the statistical analysis of the instantaneous velocities (Fig. 5, *b* and *c*), show that one-headed kinesin fragments are capable of moving at the same order of velocity as two-headed fragments during the transient moving phase.

In terms of physiological functions, however, the poor processivity of one-headed fragments (travel distance on average of 30–60 nm) would be practically useless for cellular motility such as vesicle and organelle transport. The coordination of the two heads in a hand-over-hand fashion would be required for the effective transport over long distances. In this context, the hand-over-hand mechanism may be the system by which the basal motors perform effective transport rather than the elementary process for motility.

Comparison with other studies

Several research groups have examined single-motor motility of one-headed kinesin molecules prepared from conventional two-headed kinesin (Berliner et al., 1995; Young et al., 1998; Hancock and Howard, 1998; Vale et al., 1996; Pierce et al., 1999; Okada and Hirokawa, 1999). The majority of these studies reported that, in the presence of ATP, association-dissociation events of single one-headed kinesin molecules were hardly ever observed due to a weak affinity of one-headed fragments to the microtubules.

In the present study, the affinity ($1/K_{0.5(MT)}$) of one-headed fragments was not necessarily lower than that of two-headed ones (Table 1), and the durations of the interactions were on the same order of magnitude as the two-headed fragments (Fig. 4). For K351, the duration of interaction was >3-fold longer than that reported in previous studies (Okada and Hirokawa, 1999, 2000). Thus, we were able to observe and analyze the association-dissociation events of one-headed fragments. Because it has been reported that mutations in a few amino acid sequences dramatically changes the kinesin-MT affinity (Jiang et al., 1997; Okada and Hirokawa, 2000), these affinity differences could arise from differences in either the kinesin source or the linkers for introducing reactive cysteine and fusion proteins.

In another report, Hancock and Howard (1998, 1999) reported that association-dissociation events of single one-headed kinesin molecules could be observed, but no movement was detected. Their reports, however, are not necessarily inconsistent with our result in that one-headed kinesin is less processive than two-headed kinesin, because they did not statistically analyze small displacements of the one-headed construct.

Enhanced processivity of K351BDTC

When K351 was fused at its C-terminus with BDTC, most of K351BDTC molecules (the moving fraction: 66%) moved smoothly along an ~500-nm length of microtubule.

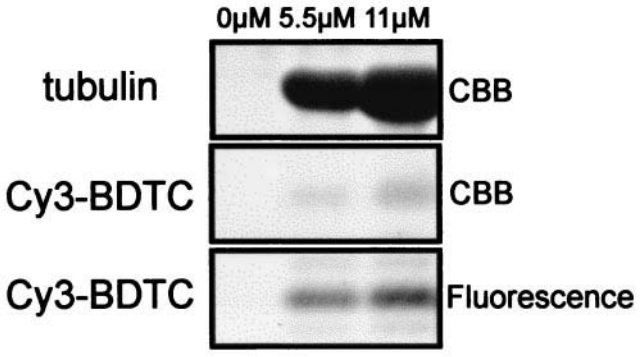

FIGURE 8 Direct binding of Cy3-BDTC to microtubules. Cy3-BDTC at 10 μM (Cy3/peptide = 1.0) was mixed with 0, 5.5, and 11 μM of microtubules (the concentration is shown by tubulin dimers) and then centrifuged. SDS-PAGE of the pellet fractions is shown. In the upper panel, tubulin (~55 kDa) was stained with Coomassie Brilliant Blue. In the middle panel, Cy3-BDTC (~18kDa) that bound to the microtubules was stained with Coomassie Brilliant Blue. In the lower panel, the fluorescence of Cy3-BDTC was examined before staining.

Duration of interaction, velocity, and travel distance for K351 all increased after fusion of BDTC, and movement in the backward direction was hardly ever observed. Thus, BDTC greatly enhanced the motility of K351. As discussed above, this enhancement cannot be explained by dimerization of K351BDTC on the microtubules. One explanation for the enhancement is that BDTC increases the affinity of one-headed kinesin molecules by interacting directly with the microtubules.

To test this possibility, we prepared Cy3-BDTC, a BDTC fragment labeled with Cy3 at the N-terminus (see Materials and Methods). When the binding of this Cy3-BDTC to microtubules was tested by co-sedimentation analysis, Cy3-BDTC co-precipitated with the microtubules (Fig. 8). The microtubule concentration, at which half the fraction of BDTC was bound, was ~30 μM. Binding of single Cy3-BDTC molecules to microtubules was also confirmed using total internal reflection fluorescence microscopy at a Cy3-BDTC concentration of 5 nM (data not shown). The binding of BDTC was also consistent with the following results. In the ATPase measurements, the affinity of K351BDTC for microtubules ($1/K_{0.5(MT)}$) was increased by eightfold as compared with that of K351 (Table 1). In the single-motor motility assay, the diffusion coefficients for K351BDTC were threefold smaller than K340 and K351. These results suggest that the direct interaction between the microtubule and BDTC prevents kinesin from diffusing away from the microtubules, while allowing its one-dimensional movement along the microtubule.

The function of BDTC for K351 may be analogous to the K-loop of KIF1A, a monomeric kinesin subfamily protein (Okada and Hirokawa, 1999). The weak, electrostatic interaction between the positively charged K-loop (lysine-rich loop 12) of KIF1A and the negatively charged E-hook (glutamate-

rich, C-terminal region) of tubulin is thought to function as an anchor for its single-headed processivity (Okada and Hirokawa, 2000; Kikkawa et al., 2000). It has also been reported that diffusional restriction by optical tweezers can stabilize the motility of one-headed K340 and K351, enabling them to make successive multiple steps of 8 nm (Inoue et al., 1997). Taking these results together, we conclude that the stability of the kinesin-MT interaction may be the key factor responsible for the processive movement of kinesin. Whatever stabilizes this interaction, whether it is the K-loop, BDTC, optical tweezers, or the two-headed coordination of the natural two-headed kinesin, may be responsible for increasing this processive movement.

We thank the members of Single Molecule Processes Project for valuable discussions and Dr. Jan West for critical reading of the manuscript.

REFERENCES

Berliner, E., E. C. Young, K. Anderson, H. K. Mahtani, and J. Gelles. 1995. Failure of a single-headed kinesin to track parallel to microtubule protofilaments. *Nature.* 373:718–721.

Block, S. M., L. S. Goldstein, and B. J. Schnapp. 1990. Bead movement by single kinesin molecules studied with optical tweezers. *Nature.* 348: 348–352.

Bloom, G. S., and S. A. Endow. 1995. Motor Proteins, Vol. 1. Academic Press, London.

Case, R. B., D. W. Pierce, N. Hom-Booher, C. L. Hart, and R. D. Vale. 1997. The directional preference of kinesin motors is specified by an element outside of the motor catalytic domain. *Cell.* 90:959–966.

Correia, J. J., Gilbert, S. P., Moyer, M. L. and Johnson, K. A. 1995 Sedimentation studies on the kinesin motor domain constructs K401, K366, and K341. *Biochemistry.* 34:4898–4907.

Cross, R. A. 1995. On the hand-over-hand footsteps of kinesin heads. *J. Muscle Res. Cell Motil.* 16:91–94.

Endow, S. A., and K. W. Waligora. 1997. Determinants of kinesin motor polarity. *Science.* 281:1200–1201.

Funatsu, T., Y. Harada, M. Tokunaga, K. Saito, and T. Yanagida. 1995. Imaging of single fluorescent molecules and individual ATP turnovers by single myosin molecules in aqueous solution. *Nature.* 374:555–559.

Hackney, D. D. 1994. Evidence for alternating head catalysis by kinesin during microtubule-stimulated ATP hydrolysis. *Proc. Natl. Acad. Sci. U.S.A.* 91:6865–6869.

Hackney, D. D. 1995. Highly processive microtubule-stimulated ATP hydrolysis by dimeric kinesin head domains. *Nature.* 377:448–450.

Hancock, W. O., and J. Howard. 1998. Processivity of the motor protein kinesin requires two heads. *J. Cell. Biol.* 140:1395–1405.

Hancock, W. O., and J. Howard. 1999. Kinesin's processivity results from mechanical and chemical coordination between the ATP hydrolysis cycles of the two motor domains. *Proc. Natl. Acad. Sci. U.S.A.* 96:13147–13152.

Harada, Y., K. Sakurada, T. Aoki, D. D. Thomas, and T. Yanagida, 1990. Mechanochemical coupling in actomyosin energy transduction studied by in vitro movement assay. *J. Mol. Biol.* 216:49–68.

Henningsen, U., and M. Schliwa. 1997. Reversal in the direction of movement of a molecular motor. *Nature.* 389:93–96.

Higuchi, H., E. Muto, Y. Inoue, and T. Yanagida. 1997. Kinetics of force generation by single kinesin molecules activated by laser photolysis of caged ATP. *Proc. Natl. Acad. Sci, U.S.A.* 94:4395–4400.

Howard, J., A. J. Hudspeth, and R. D. Vale. 1989. Movement of microtubules by single kinesin molecules. *Nature.* 342:154–158.

Hua, W., E. C. Young, M. L. Fleming, and J. Gelles. 1997. Coupling of kinesin steps to ATP hydrolysis. *Nature.* 388:390–393.

Huang, T-G., and D. Hackney. 1994. *Drosophila* kinesin minimal motor domain expressed in *Escherichia coli*. *J. Biol. Chem.* 269:16493–16501.

Huang, T-G., J. Suhan, and D. Hackney. 1994. *Drosophila* kinesin motor domain extending to amino acid position 392 is dimeric when expressed in *Escherichia coli. J. Biol. Chem.* 269:16493–16501.

Hyman, A., D. Drechsel, D. Kellogg, S. Salser, K. Sawin, P. Steffen, L. Wordeman, and T. Mitchison. 1991. Preparation of modified tubulins. *Methods Enzymol.* 196:478–485.

Inoue, Y., Y. Y. Toyoshima, A. H. Iwane, S. Morimoto, H. Higuchi, and T. Yanagida. 1997. Movements of truncated kinesin fragments with a short or an artificial flexible neck. *Proc. Natl. Acad. Sci. U.S.A.* 947275–7280.

Iwane, A. H., K. Kitamura, M. Tokunaga, and T. Yanagida. 1997. Myosin subfragment-1 is fully equipped with factors essential for motor function. *Biochem. Biophys. Res. Commun.* 230:76–80.

Iwatani, S., A. H. Iwane, H. Higuchi, Y. Ishii, and T. Yanagida. 1999. Mechanical and chemical properties of cysteine-modified kinesin molecules. *Biochemistry.* 38:10318–10323.

Jiang, W., M. F. Stock, X. Li, and D. D. Hackney. 1997. Influence of the kinesin neck domain on dimerization and ATPase kinetics. *J. Biol. Chem.* 272:7626–7632.

Kikkawa, M., Y. Okada, and N. Hirokawa. 2000. 15 Å resolution model of the monomeric kinesin motor, KIF1A. *Cell.* 100:241–252.

Kozielski, F., S. Sack, A. Marx, M. Thormahlen, E. Schonbrunn, V. Biou, A. Thompson, E. M. Mandelkow, and E. Mandelkow. 1997. The crystal structure of dimeric kinesin and implications for microtubule-dependent motility. *Cell.* 91:985–994.

Kull, F. J., E. P. Sablin, R. Lau, R. J. Fletterick, and R. D. Vale. 1996. Crystal structure of the kinesin motor domain reveals a structural similarity to myosin. *Nature.* 380:550–555.

Ma, Y-Z., and E. W. Taylor. 1997. Kinetic mechanism of a monomeric kinesin construct. *J. Biol. Chem.* 272:717–723.

Miyamoto, Y., Muto, E., Mashimo, T., Iwane, A. H., Yoshiya, I., and Yanagida. T. 2000. Direct inhibition of microtubule-based kinesin motility by local anesthetics. *Biophys. J.* 78:940–949.

Moyer, M. L., S. P. Gilbert, and K. A. Johnson. 1996. Purification and characterization of two monomeric kinesin constructs. *Biochemistry.* 35:6321–6329.

Okada, Y., and N. Hirokawa. 1999. A processive single-headed motor: kinesin superfamily protein KIF1A. *Science.* 283:1152–1157.

Okada, Y., and N. Hirokawa. 2000. Mechanism of the single-headed processivity: Diffusional anchoring between the K-loop of kinesin and the C terminus of tubulin. *Proc. Natl. Acad. Sci. U.S.A.* 97:640–645.

Pierce, D. W., N. Hom-Booher, A. J. Otsuka, and R. D. Vale. 1999. Single-molecule behavior of monomeric and heteromeric kinesins. *Biochemistry.* 38:5412–5421.

Rice, S., A. W. Lin, D. Safer, D. S. Hart, N. Naber, B. O. Carragher, S. M. Cain, E. Pechatnikova, E. M. Wilson-Kubalek, M. Whittaker, E. Pate, R. Cooke, E. W. Taylor, R. A. Milligan, and R. D. Vale. 1999. A structural change in the kinesin motor protein that drives motility. *Nature.* 402: 778–784.

Romberg, L., D. W. Pierce, and R. D. Vale. 1998. Role of the kinesin neck region in processive microtubule-based motility. *J. Cell. Biol.* 140: 1407–1416.

Sack, S., J. Muller, A. Marx, M. Thormahlen, E. M. Mandelkow, S. T. Brady, and E. Mandelkow. 1997. X-ray structure of motor and neck domains from rat brain kinesin. *Biochemistry.* 36:16155–16165.

Schnitzer, M. J., and S. M. Block. 1997. Kinesin hydrolyses one ATP per 8-nm step. *Nature.* 388:386–390.

Vale, R. D., T. Funatsu, D. W. Pierce, L. Romberg, Y. Harada, and T. Yanagida. 1996. Direct observation of single kinesin molecules moving along microtubules. *Nature.* 380:451–453.

Vugmeyster, Y., E. Berliner, and J. Gelles. 1998. Release of isolated single kinesin molecules from microtubules. *Biochemistry.* 37:747–757.

Young, E. C., H. K. Mahtani, and J. Gelles. 1998. One-headed kinesin derivatives move by a nonprocessive, low-duty ratio mechanism unlike that of two-headed kinesin. *Biochemistry.* 37:3467–3479.